Accelerated Publications

Microsomal Triglyceride Transfer Protein Is Required for Yolk Lipid Utilization and Absorption of Dietary Lipids in Zebrafish Larvae†

Amnon Schlegel*,‡,§ and Didier Y. R. Stainier‡,||

Department of Biochemistry and Biophysics, Department of Medicine, Division of Endocrinology, and UCSF Programs in Developmental Biology, Genetics and Human Genetics, and the Liver Center, University of California, MC-2711, 1550 Fourth Street, Room 381, San Francisco, California 94143

Received September 15, 2006; Revised Manuscript Received November 13, 2006

ABSTRACT: Although the absorption, transport, and catabolism of dietary lipids have been studied extensively in great detail in mammals and other vertebrates, a tractable genetic system for identifying novel genes involved in these physiologic processes is not available. To establish such a model, we monitored neutral lipid by staining fixed zebrafish larvae with oil red o (ORO). The head structures, heart, vasculature, and swim bladder stained with ORO until the yolk was consumed 6 days after fertilization (6 dpf). Thereafter, the heart and vasculature no longer had stainable neutral lipids. Following a high-fat meal, ORO stained the intestine and vasculature of 6 dpf larvae, and whole-larval triacylglycerol (TAG) and apolipoprotein B levels increased. Levels of microsomal triglyceride transfer protein (Mtp), the protein responsible for packaging TAG and betalipoproteins into lipoprotein particles, were unchanged by feeding. Since the developing zebrafish embryo expresses *mtp* in the yolk cell layer, liver, and intestine, we determined the effect of targeted knockdown of Mtp expression using an antisense morpholino oligonucleotide approach (Mtp MO) on the transport of yolk and dietary lipids. Mtp MO injection led to loss of Mtp expression and of lipid staining in the vasculature, heart, and head structures. Mtp MO-injected larvae were smaller than age-matched, uninjected larvae, consumed very little yolk, and did not absorb dietary neutral lipids; however, they absorbed a short chain fatty acid that does not require Mtp for transport. Importantly, the vasculature appeared unaffected in Mtp MO-injected larvae. These studies indicate that zebrafish larvae are suitable for genetic studies of lipid transport and metabolism.

Since derangements in the uptake, transport, and disposition of neutral lipids underlie several diseases such as obesity, hyperlipidemia, atherosclerosis, hepatic steatosis, and diabetes mellitus, a tractable genetic system for identifying novel genes involved in these physiologic processes is needed. The absorption, transport, and catabolism of dietary lipids have been studied in molecular detail in mammals and other vertebrates. Medium and long chain fatty acids liberated from phospholipids and triacylglycerol (TAG)[1] by luminal lipases are taken up by the intestinal epithelium through fatty acid transport proteins (*1*). Fatty acids are activated to acyl coenzyme A (AcSCoA) by long chain fatty acyl coenzyme A synthases (*2*). AcSCoA moieties are carried by fatty acid binding proteins (*3*) and are used as building blocks for the production of TAG and cholesterol esters through the action of various acyl transferases (*4*). TAG, cholesterol esters of fatty acids, free cholesterol, and phospholipids are combined with apolipoprotein B-48 (Apob-48) in the endoplasmic reticulum lumen through the actions of microsomal triglyceride transfer protein (Mtp) and its multifunctional partner protein disulfide isomerase (Pdi) to form nascent chylomicrons (*5*−*7*). These particles travel through the secretory pathway and are released from the basolateral surface of the enterocyte into the lymphatic system (*7*). A similar packaging of neutral lipids and Apob-100 occurs in the liver for the generation of very low-density lipoprotein (VLDL) particles.

The lipid transport machinery is ancient. The central proteins are not only evolutionarily conserved among species; several of them (vitellogenins, apolipophorin-II/I, Apob, and CD1) are encoded by genes that share a common ancestor, *mtp* (*7*). Highlighting this conservation, lipoprotein particle processing can be reconstituted in vitro using proteins from different species (*8*−*10*). This high degree of conservation in the machinery of lipid transport makes genetic studies in zebrafish very attractive for uncovering regulatory processes: zebrafish larvae express *mtp* in the yolk cell layer, intestine, and liver (*11*).

† This work was supported by a Sandler Family Supporting Foundation Opportunity Award in Basic Sciences.

* To whom correspondence should be addressed. Telephone: (415) 502-4381. Fax: (415) 476-3892. E-mail: amnon.schlegel@ucsf.edu.

‡ Department of Biochemistry and Biophysics.

§ Department of Medicine, Division of Endocrinology.

|| UCSF Programs in Developmental Biology, Genetics and Human Genetics, and the Liver Center.

[1] Abbreviations: AcSCoA, acyl coenzyme A; Apob, apolipoprotein B; BODIPY 558/568 C12, 4,4-difluoro-5-(2-thienyl)-4-bora-3a,4a-diaza-*s*-indacene-3-dodecanoid acid; dpf, days postfertilization; GFP, green fluorescent protein; MO, morpholino nucleic acid; Mtp, microsomal triglyceride transfer protein; ORO, oil red o; Pdi, protein disulfide isomerase; Pgc1, peroxisome-proliferator-activated receptor γ coactivator 1; TAG, triacylglycerol.

10.1021/bi0619268 CCC: $33.50
Published on Web 12/01/2006

In addition to expressing the key components of the transport machinery (*11*, *12*) and using evolutionarily conserved lipoproteins (*13*−*15*), the zebrafish embryonic intestine is metabolically active: enterocytes package meal-derived lipids into lipoprotein particles for absorption into the circulation (*15*). Because the zebrafish larva is transparent, the metabolic activity of its intestine (e.g., the action of phospholipase A_2) can be directly visualized with fluorescent lipid analogues (*12*, *16*). Furthermore, similar to mature mouse intestine, gut flora elicit global changes in zebrafish embryonic intestine gene expression, including upregulation of *apob* (*17*). These properties have been exploited in a genetic screen in zebrafish to identify a mutant that fails to absorb a fluorescent analogue of valeric acid (BODIPY C5); the isolated gene encodes a Golgi structural protein whose mutation results in enterocyte, biliary epithelial, and exocrine pancreatic epithelial secretory dysfunction (*16*, *18*). A similar screen in medaka larvae identified several mutants that fail to process BODIPY C5 (*19*).

While fluorescently conjugated fatty acids are transported from the extracellular space using the very machinery that transports untagged fatty acids (*20*), fluorescent analogues of fatty acids are minimally incorporated into neutral lipids (*21*), making them suitable for study of some (*17*−*19*) but not all components of dietary lipid metabolism. For instance, fluorescently conjugated fatty acids have never been seen in the circulation of zebrafish. Similar observations have been made in adult *Caenorhabditis elegans* whose intestinal lipid stores can be stained with fluorescently labeled fatty acids (*22*). Although the concentration of such dyes may be too low to allow such visualization in the vasculature of fish larvae, when the yolks of medaka embryos were injected with BODIPY and several other polyaromatic dyes shortly after fertilization, the dyes were found to concentrate preferentially in the gall bladder when the animals reached the larval stage (*23*). Thus, developing fish larvae treat these dyes as metabolic waste and excrete them through the hepatobiliary system (*23*). In summary, fluorescent dyes are excellent probes of biliary transport (*17*−*19*, *23*) but are not ideal for studying all steps of lipid transport.

To visualize neutral lipid throughout the developing organism, we stained fixed zebrafish embryos and larvae with oil red o (ORO) during the first week of life. We also monitored lipid absorption following feeding of high-fat liquid with this stain. Next, we determined the suitability of this lipid staining method for use in genetic studies by examining the effect of knocking down Mtp expression with antisense morpholino oligonucleotides (MO). Our findings in zebrafish larvae parallel the most severe findings seen in human abetalipoproteinemia, which is caused by mutations in *MTP* (*24*, *25*), and are similar to those for the phenotype of $Mtp^{-/-}$ mice (*26*−*29*).

EXPERIMENTAL PROCEDURES

Fish Stocks. Fish were maintained using standard methods (*30*). *Tg(gut:GFP)*^{s854}, *Tg(flk1:GFP)*^{s843}, and *cloche* fish were described previously (*31*−*33*). WT fish were from the Tübingen stock.

MO Injections. Single-cell embryos were injected with the Mtp translation-inhibiting MO 5′-CGGCAACCGGCAT-CATAGTTTAGGG (1 ng/embryo).

Feeding Experiments. Larvae were placed in embryo water containing a 1:10 dilution of heavy whipping cream (Clover Stornetta Farms, final fat concentration of 40 g/L) for 1−6 h at 28 °C.

Fluorescence Imaging. Larvae were placed in 100 nM fluorescently tagged lauric acid [4,4-difluoro-5-(2-thienyl)-4-bora-3a,4a-diaza-*s*-indacene-3-dodecanoid acid, BODIPY 558/568 C12, Molecular Probes] or 0.1 mg/L nile red (Sigma) for 1 h at 28 °C. In experiments using the fluorophore PED6 (*16*), 4-day-old WT or Mtp MO-injected larvae were incubated for 24 h at 28 °C with 250 nM PED6.

Oil Red o Staining. Embryos and larvae were fixed in PBS and 3.7% formaldehyde for 6−12 h at 4 °C, washed, and stained with filtered 0.3% ORO in 60% 2-propanol for 2 h. After a final wash in PBS, organisms were placed in depression wells and photographed.

Antibodies and Immunoblotting. Protein extracts were prepared by placing equal numbers (typically 40−70) of larvae in 0.5 mL of lysis buffer [50 mM Tris (pH 8.0), 150 mM NaCl, 1% Triton X-100, and 0.1% SDS] containing a cocktail of protease inhibitors (Complete MINI, Roche) and sonicating them for 10 s. Insoluble materials were removed by centrifugation. Proteins were separated by SDS−PAGE (8% acrylamide) under reducing conditions, transferred to nitrocellulose membranes, and stained with Ponceau S. Goat anti-mouse apoB 48/100 IgG was from Biodesign International. Mtp was detected with a rabbit anti-human MTP−PDI heterodimer IgG kindly provided by C. C. Shoulders (*34*); zebrafish Pdi was not detected with this IgG, by rabbit anti-PDI IgG (SPA-890) from Stressgen Bioreagents, or by mouse monoclonal anti-PDI from BD Pharmingen (*35*). HepG2 PDI and Mtp were detected with the rabbit anti-human MTP−PDI heterodimer IgG and by mouse monoclonal anti-Mtp and anti-PDI IgGs from BD Pharmingen. Goat anti-Foxa2 and rabbit anti-β-tubulin IgGs were from Abcam. Rabbit anti-PGC1 IgG was from Calbiochem. Donkey anti-goat and goat anti-rabbit polyclonal IgG−HRP antibodies were from Santa Cruz Biotechnology. Rabbit anti-mouse IgG-HRP was from Zymed. An enhanced chemiluminescent substrate (Pierce) was used to detect HRP activity.

Triacylglycerol Assay. After being extensively washed to remove unconsumed fat, larvae were transferred to a tight fitting 7 mL Dounce homogenizer. Water was removed, and the larvae were homogenized with 0.5 mL of a 2:1 (v/v) cholorform/methanol solution. The mixture was dried under nitrogen, and lipids were separated by thin layer chromatography (Whatman Particil LK6D) using an 80:20:1 (v/v/v) mixture of hexane, ethyl ether, and acetic acid as the resolving agent. Glyceryl trioleate (Sigma) standards were run in parallel. TAG was scraped from the plates after resolution and analyzed using a perchlorate reagent (*36*). First, 0.5 mL of hydroxylamine reagent was added to the purified TAG samples. The samples were incubated at 65 °C for 2 min, cooled for 5 min, and then incubated with 2.5 mL of freshly prepared perchlorate reagent. Thirty minutes later, the absorbance was read at 530 nm. The absorbance of the glyceryl trioleate standards was used to generate a curve from which the masses of TAG in the samples were interpolated. Hydroxylamine reagent was prepared by combining equal volumes of hydroxylamine (4%, w/v) dissolved in ethanol (95%, v/v) and NaOH (8%, w/v) dissolved in ethanol (95%, v/v) and then removing the precipitated NaCl

by centrifugation. Ferric perchlorate stock solutions were prepared by dissolving 5 g of $Fe(ClO_4)_3$ in 10 mL of concentrated $HClO_4$ (70%, w/v) and 10 mL of water and then diluting to a final volume of 100 mL with absolute ethanol. Perchlorate reagent was made by adding 4 mL of the stock $Fe(ClO_4)_3$ solution with 3 mL of concentrated $HClO_4$ and diluting to a final volume of 100 mL with ethanol (95%, v/v). Results are reported as the mean ± the standard deviation of three independent experiments run in parallel. Unpaired, two-sided Student's *t*-tests were performed to compare the TAG content. Statistical significance was taken as $P < 0.05$.

Cell Culture. HepG2 cells were cultured in minimal essential medium supplemented with fetal calf serum (10%), nonessential amino acids, and sodium pyruvate. After two washes in PBS, cells (one confluent 10 cm diameter dish) were incubated in serum-free medium (10 mL) containing 200 μM naringenin (*37*) or vehicle (DMSO) for 6 h. Secreted proteins were precipitated from the medium by adjusting an aliquot (2 mL) of the medium to 10% trichloroacetic acid. Following centrifugation, precipitated proteins were resuspended directly into SDS−PAGE loading buffer. A cellular protein lysate was prepared as described above.

RESULTS

Minimal Intestinal Absorption of a Fluorescently Labeled Medium Chain Fatty Acid. Fluorescently labeled valeric acid (BODIPY C5) is absorbed by the intestine of zebrafish larvae and undergoes prompt hepatobiliary transport, culminating in concentration in the gall bladder (*17*). Because fatty acids with chain lengths of 10 or more carbon atoms require incorporation into TAG and packaging into a lipoprotein particle for absorption by teleosts specifically (*38*) and eukaryotes more generally (*1*, *20*), we determined whether BODIPY-conjugated lauric acid (12 carbons) was absorbed in the same manner as BODIPY C5 in the hopes of developing a probe for lipoprotein transport. When photographed 2 or 6 h after a 1 h incubation with BODIPY 558/568 C12, 5 day postfertilization (dpf) *Tg(gut:GFP)*^{s854} larvae (*31*), which express green fluorescent protein (GFP) throughout the digestive system (including the intestine, liver, biliary system and gall bladder, and pancreas), exhibited strong lipid fluorescence in the intestine, although yolk autofluorescence was also apparent at this stage (Figure 1). When BODIPY 558/568 C12 was fed to 6 dpf larvae, the intestine was labeled but yolk autofluorescence was no longer present (Figure 1).

Rarely (three of 101 larvae), we saw BODIPY 558/568 C12 in the gall bladder of 6 dpf larvae, indicating that this fatty acid analogue can be absorbed by the intestine, taken up by the liver, and secreted into the biliary system; however, the efficiency of this transport is very poor in comparison to that of BODIPY C5 (*17*). The vital, neutral lipid stain nile red also labeled the anterior intestine strongly and was occasionally found in the gall bladder (seven of 94 larvae), indicating that it was also absorbed and subjected to hepatobiliary excretion. Panels m and n of Figure 1 show larvae that concentrate BODIPY 558/568 and nile red in the gall bladder, respectively.

Lipid Utilization during Embryogenesis. Since BODIPY 558/568 C12 and nile red were mostly seen in the intestine after feeding, we fixed and stained whole larvae with the neutral lipid stain ORO to examine the location of neutral lipids in other organs. By 2 dpf, the head and heart of developing zebrafish embryos and larvae stain with ORO (*39*); however, the location of neutral lipids later in development is unknown. As shown in Figure 2, from 2 to 5 dpf, the yolk stained with ORO, as did head structures, the swim bladder, the heart, and what appeared to be the vasculature. Once the yolk's neutral lipid was completely consumed, the vascular and heart staining disappeared, but the swim bladder continued to stain with ORO. To confirm that the vasculature was stained with ORO, we compared ORO staining in wild-type (WT) and *cloche* mutant larvae, which lack blood cells and a vasculature (*33*). To allow direct visual comparison, we used *Tg(flk1:EGFP)*^{s843} larvae, which express enhanced GFP under the control of the vascular endothelial growth factor receptor 2 promoter (*32*). As shown in Figure 2, *cloche* mutants did not demonstrate the intersegmental ORO staining seen in WT larvae from 2 to 5 dpf, suggesting that the intersegmental ORO staining occurs in blood vessels. We could not analyze 5 dpf *cloche* mutant larvae because they were generally in very poor shape with pronounced edema. Thus, ORO staining can be used to monitor endotrophic (i.e., yolk-derived) lipid consumption during the embryonic and early larval stages. Interestingly, swim bladder ORO staining was present in *cloche* mutants (panel p in Figure 2), indicating that this organ's concentration of neutral lipids (presumably for surfactant production) does not require an intact vasculature.

Lipid Staining following High-Fat Feeding. To assess whether ORO staining could be used to monitor dietary lipid absorption, we examined 6 dpf larvae following feeding of a high-fat liquid. After incubation for 1 h in a 4% solution of fat, the anterior intestine of 6 dpf larvae stained with ORO

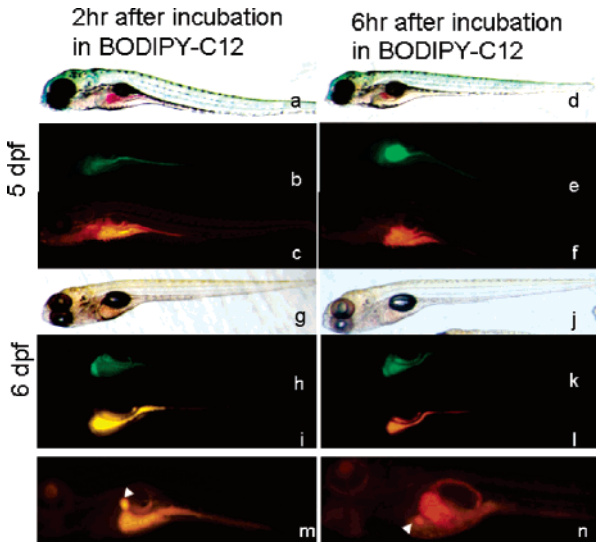

FIGURE 1: Minimal absorption of a fluorescently medium chain fatty acid analogue. Five (a−f) or 6 dpf (h−l) larvae expressing GFP throughout the digestive system (b, e, h, and k) were incubated with 100 nM BODIPY C12 for 2 or 6 h. Light (a, d, g, and j) and red fluorescence micrographs (c, f, i, and l) were taken. Note that 5 dpf larvae exhibited residual yolk autofluorescence (c and f) under the red filter, in addition to intestinal labeling. Rarely (three of 101 larvae), BODIPY C12 was seen in the gall bladder (m). This minimal absorption was similar to that seen for nile red: seven of 94 larvae exhibited the gall bladder concentration of this dye (as in panel n).

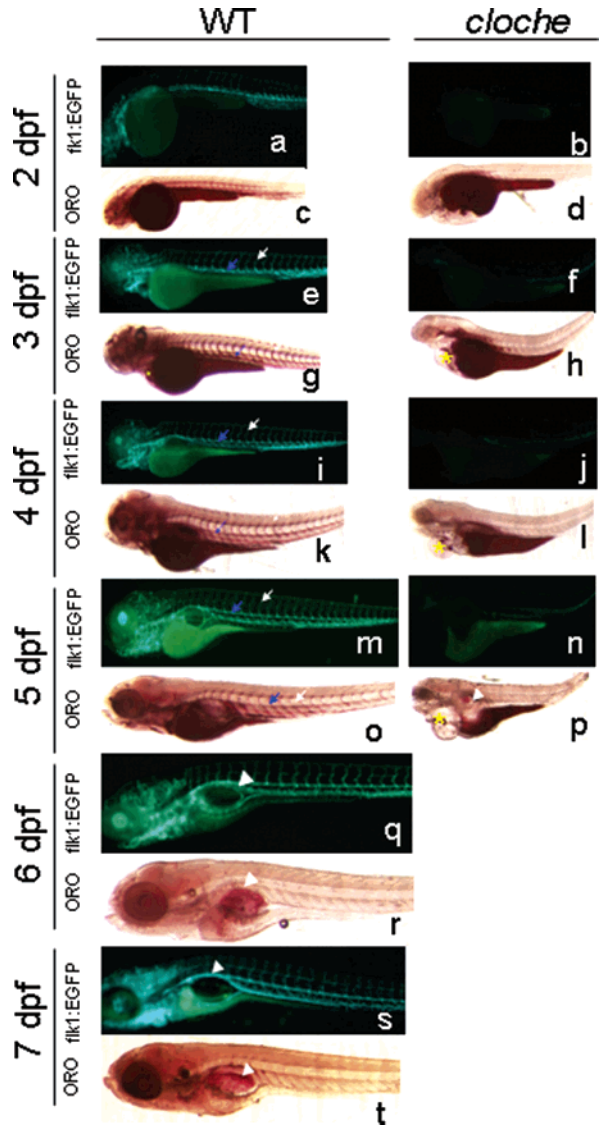

FIGURE 2: Tracking endotrophic lipid consumption in whole larvae. WT and *cloche* mutant larvae expressing EGFP under the control of vascular endothelial growth factor receptor 2 (flk1:EGFP) were photographed under green fluorescent filters (a, b, e, f, i, j, m, n, q, and s) before fixation and staining with ORO (c, d, g, h, k, l, o, p, r, and t). Two (a−d), 3 (e−h), 4 (i−l), 5 (m−p), 6 (q and r), and 7 (s and t) dpf organisms are shown. Note the progressive decrease in the neutral lipid seen in the yolk, with the complete absence of staining by 6 dpf in WT larvae (c, g, k, o, and r). The dorsal aorta (blue arrows) and intersegmental vessels (white arrows) stained for neutral lipid through 5 dpf. In addition to the staining of the head structures, the developing heart was stained with ORO from 2 to 5 dpf (asterisk). Once the yolk was completely consumed, strong ORO staining remained only in the swim bladder (arrowheads). Note, *cloche* mutants did not have similar intersegmental ORO staining, but the swim bladder did stain with ORO (p).

(Figure 3A). After the larvae had been fed for 6 h, the intersegmental vessels also exhibited strong staining with ORO (Figure 3A).

The increase in the level of ORO staining following high-fat feeding correlated with whole-larval TAG levels (Figure 3B). The fasting TAG level in 6 dpf larvae was approximately 2.5 times higher than that previously reported in 72 h postfertilization larvae that were deyolked 1 h prior to analysis (*40*). A statistically significant increase in TAG levels was seen after incubation for both 1 and 6 h in high-fat liquid. These quantitative results corroborate the qualitative increase seen with ORO staining.

Larvae fed for 6 h and then placed in water for an additional 18 h prior to fixation no longer exhibited vascular lipid staining, although the amount of residual intestinal staining varied (Figure 3C), with 72 of 114 showing no residual lipid (Figure 3C, panels c and d), 27 of 114 showing faint residual intestinal lipid staining (Figure 3C, panels e and f), and 15 of 114 showing strong residual intestinal staining (Figure 3C, panels g and h). Importantly, those larvae showing residual intestinal staining had minimal staining of the vasculature 18 h after feeding. Thus, ORO staining can be used to monitor diet-derived lipid consumption, absorption, and transport in the zebrafish larvae.

Dietary Control of Mtp Protein Levels. In response to a single high-fat meal, *mtp* mRNA levels in the proximal intestine and liver of zebrafish larvae increase (*11*). This observation is similar to those made in several other systems. For instance, similar upregulation of hamster liver *Mtp* mRNA levels occurs in response to high-fat and high-cholesterol feeding (*41*, *42*). Modest changes in *Mtp* mRNA levels are seen in an immortalized cell line derived from swine intestine in response to incubation with various long chain fatty acids, although protein levels are minimally altered (*43*). Likewise, small but statistically significant changes are seen in hamster intestinal Mtp protein levels in response to chronic high-fat and high-sucrose feeding (*44*). Finally, high-fat feeding of mice for 21 days results in an increased level of expression of Mtp in the distal small intestine (*45*).

To address whether changes in zebrafish *mtp* mRNA following high-fat feeding result in an increased level of protein expression, we performed immunoblot analyses on whole-larval extracts of fed and fasted 6 dpf larvae using antisera raised in rabbits against purified, recombinant human Mtp−Pdi heterodimers (*34*). Mtp protein levels did not change after a 1 or 6 h feeding (Figure 3D). This difference between mRNA and protein levels is consistent with findings in an immortalized enterocyte cell line (*43*), hamster liver (*41*, *42*), and intestines (*45*): short-term feeding has no effect on Mtp protein levels. Indeed, upregulation of Mtp protein in the mouse intestine is seen after only 3 weeks of high-fat feeding (*45*). This discrepancy between the message and product of the *mtp* gene may reflect increased *mtp* mRNA stability or increased prandial Mtp degradation despite stronger synthesis. As expected, Apob levels increased in response to feeding, with the detection of a single Apob species at baseline, and the production of two bands after feeding, suggesting an increased level of production of Apob-100 (hepatic) and Apob-48 (intestinal) in response to the meal.

Targeted Knockdown of Mtp. Next, we determined the effect of a decreasing level of Mtp expression by injecting embryos with a translation initiation inhibiting antisense MO (Mtp MO). Similar to $Mtp^{-/-}$ mice (*26*), zebrafish larvae injected with Mtp MO consumed very little yolk, were small, and died by 6 dpf with pronounced edema (Figure 4A). Larvae injected with Mtp MO exhibited minimal head structure, heart, and vasculature staining with ORO. Immunoblot analyses of lysates prepared from 5 dpf larvae confirmed that injection of Mtp MO led to decreased Mtp protein levels (Figure 4C). When less Mtp MO was injected,

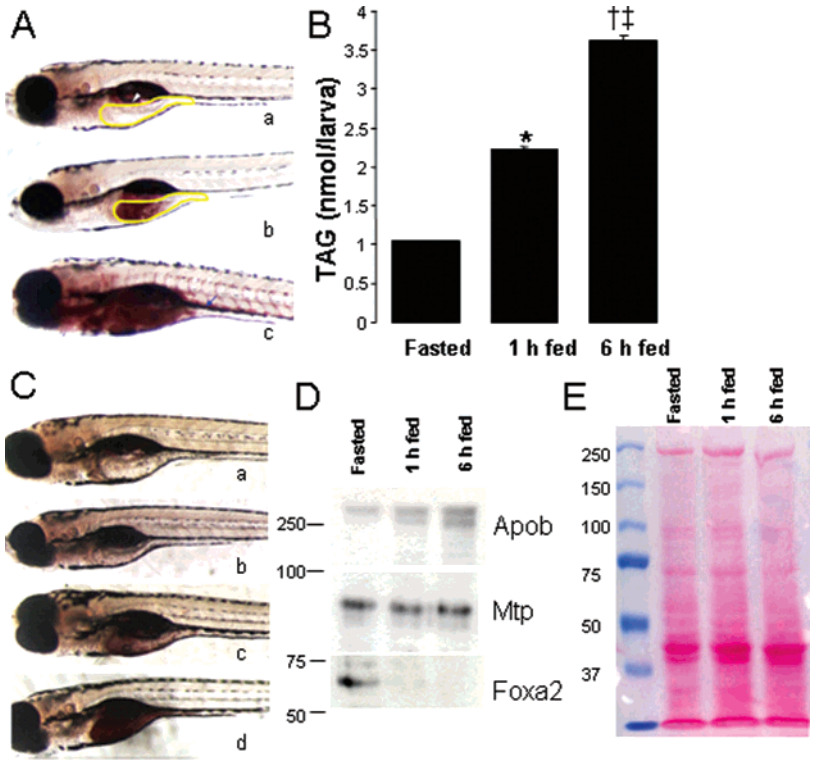

FIGURE 3: Monitoring dietary lipid absorption in whole larvae. (A) Six days postfertilization larvae were placed ("fed") in embryo medium containing heavy whipping cream for 1 (b) or 6 h (c). In parallel, larvae were maintained ("fast") in embryo medium without whipping cream (a). Note the presence of the neutral lipid in the anterior intestine (yellow outline) after 1 h and the detection of lipid in the vasculature after 6 h (dorsal aorta, blue arrow; intersegmental vessels, white arrows). The swim bladder (white arrowheads) stains with ORO in the fasting state. (B) TAG content of fed (black bars) or fasted (white bars) 6 dpf zebrafish larvae. There was a time-dependent increase in whole-larval TAG content that correlated with the increased level of ORO staining seen in panel A: (∗) $P = 0.022$ vs fasted, (†) $P = 0.019$ vs fasted, and (‡) $P = 0.030$ vs 1 h fed. (C) Six days postfertilization larvae were fed for 6 h as described for panel A, washed extensively to remove fat from the medium, and then transferred to fresh embryo water for 18 h. Larvae were then fixed and stained with ORO. Eighteen hours after the meal, there was a range of residual ORO staining in the intestinal lumen, with the majority of fed larvae exhibiting minimal (b) staining, some showing moderate ORO staining (c), and a few showing strong (d) staining. In parallel to this postmeal monitoring, larvae were maintained in water without whipping cream (a). Note that the fasted larva exhibited minimal staining with ORO except in the swim bladder. (D) Immunoblot analysis of protein extracts (15 μg/lane) prepared from larvae fed or fasted as described for panel A. Note that feeding for 1 or 6 h has no effect on whole-embryo Mtp protein levels but causes an increase in Apob levels. Foxa2 levels decreased within 1 h of feeding. (E) Ponceau S staining of the nitrocellulose membrane used in panel D.

Mtp protein levels were not altered, and no discernible phenotype was observed (not shown).

Apob levels were not altered by Mtp MO injection, likely reflecting the steady state production and subsequent degradation of unlipidated Apob (*7*). Similar to the results seen with Apob, the whole-larval levels of the very abundant yolk-derived lipoproteins vitellogenin and lipovitellin were not affected by Mtp MO injection (Figure 4C). Importantly, these yolk-derived lipoproteins are not as abundant once the yolk is completely consumed 6 pdf (Figure 3E). We confirmed this observation in a heterologous system by examining intracellular and secreted ApoB levels in cultured hepatocytes grown in the presence and absence of the Mtp inhibitor naringenin (Figure 4E). While the amount of ApoB recovered from the medium decreased when cells were treated with naringenin (*37*), the intracellular ApoB level was unaffected by naringenin. Importantly, we confirmed that a 6 h treatment with naringenin did not decrease cellular Mtp or PDI levels (Figure 4E). Thus, knockdown of zebrafish Mtp does not alter the production of apolipoproteins, similar to the findings in $Mtp^{-/-}$ mice (*26*−*28*) and cultured hepatocytes.

While the minimal consumption of yolk lipids, small body size, and pericardial edema seen in Mtp MO-injected larvae are most likely consequences of malnutrition because of the inability to transport yolk TAG, the possibility that Mtp is required for cardiovascular development remained. To formally exclude defects in vascular development as contributing to the phenotypes seen in Mtp MO-injected larvae, we examined the consequences of knocking down Mtp expression in *Tg(flk1:EGPF)* larvae. Mtp MO-injected larvae appeared unaffected (Figure 4D) and blood was seen circulating, indicating that Mtp is not required for cardiovascular development.

Recent work has identified transcription factor Foxa2 and its coactivator peroxisome-proliferator-activated receptor γ coactivator 1 (Pgc1) as important regulators of Mtp expression and VLDL secretion in mouse liver (*46*). Foxa2 but not Pgc1 levels (not detected by immunoblotting of lysates from 6 pdf larvae) decreased in response to feeding (Figure 3D), but both Foxa2 and Pgc1 levels increased in Mtp MO-injected 5 pdf larvae (Figure 4B). Thus, upregulation of the Foxa2−Pgc1 transcription factor−coactivator complex that drives *mtp* expression in the Mtp MO-injected larvae may reflect a coordinated attempt by the starving larva to increase the level of Mtp production.

After determining that Mtp MO injection downregulates Mtp expression and results in a gross phenotype marked by poor endotrophic lipid utilization, we assessed whether

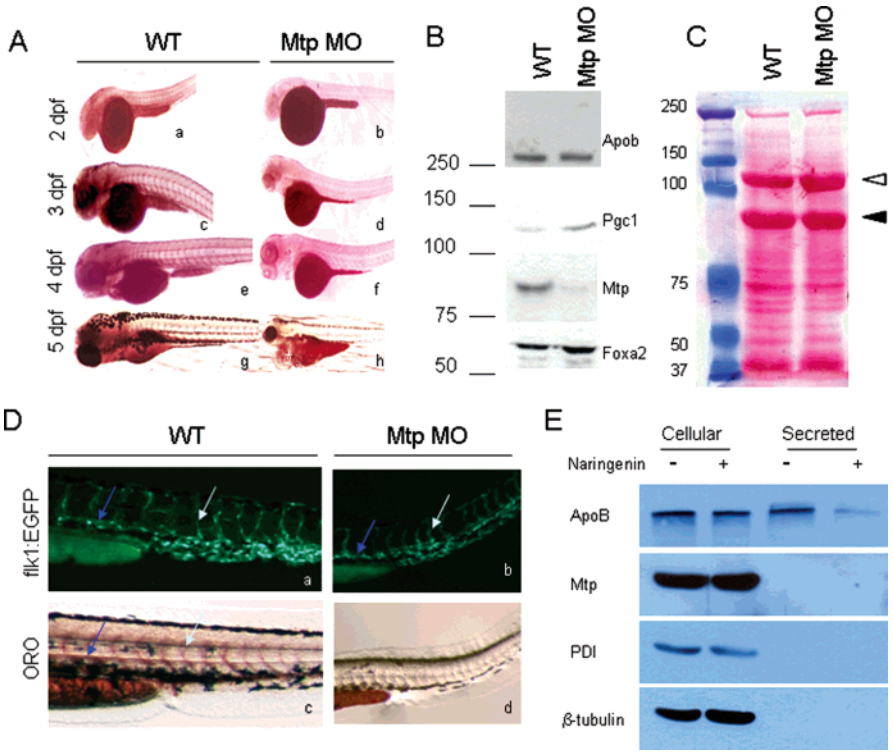

FIGURE 4: Mtp MO blocks yolk consumption. (A) Compared to 2 (a), 3 (c), 4 (e), and 5 (g) dpf WT larvae, larvae injected with Mtp MO consumed far less yolk and had minimal vascular and head structure lipid staining on 2 (b), 3 (d), 4 (f), and 5 dpf (h). Note the small size of the Mtp MO-injected larvae as well as the presence of pericardial edema (white asterisk). The vascular pattern of ORO staining seen in the WT larvae is absent in the Mtp MO-injected larvae. (B) Immunoblot analysis of extracts prepared from 5 dpf larvae shows that Mtp MO injection decreases Mtp protein levels, but levels of Apob remained constant. Both PGC1 and Foxa2 levels were increased in Mtp MO-injected larvae. (C) A Ponceau S-stained nitrocellulose membrane used in panel B shows that the very high levels of lipovitellin (white arrowhead) and vitellogenin (black arrowhead) were not affected by Mtp MO injection. (D) To confirm that Mtp MO injection does not affect vascular development, *Tg(flk1:EGFP)* larvae were injected with Mtp MO. Note the presence of the dorsal aorta (blue arrows) and intersegmental vessels (white arrows) in uninjected (a) and Mtp MO-injected (b) 3 dpf larvae, and the absence of vascular lipid staining in Mtp MO-injected larvae (d). (E) HepG2 cells incubated in medium lacking serum were treated with vehicle (DMSO) or the Mtp inhibitor naringenin for 6 h. The medium was collected, and proteins were precipitated with trichloroacetic acid from an aliquot of the medium. A protein lysate was prepared after extensive washing of the cells. Proteins were subjected to immunoblot analysis. Note that intracellular Apob levels remained constant, while the level of secretion of Apob decreased when cells were treated with naringenin. Mtp and Pdi levels remained constant during the treatment as well; β-tubulin served as a cytoplasmic protein control for equal loading.

loss of Mtp affected dietary lipid absorption. First, the transport of the short chain fatty acid analogue BODIPY C5, derived from the hydrolysis of PED6 by phospholipase A_2 in the intestinal lumen, was assessed by examining zebrafish larvae fluorescence in the gall bladder. PED6 is a phosphatidylethanolamine that contains an intramolecular quencher of the BODIPY moiety, allowing the monitoring of phospholipase A_2 activity with the detection of liberated BODIPY C5 in the intestine. Once liberated from PED6, BODIPY C5 is absorbed by the intestine, transported to the liver, and excreted into the gall bladder (*12*, *17*, *18*). As shown in Figure 5A, 5 dpf Mtp MO-injected larvae fed PED6 exhibited green fluorescence in the intestine, reflecting normal lumen hydrolysis of PED6. They also exhibited normal concentration of BODIPY C5 in the gall bladder. Thus, Mtp MO injection does not cause defects in intestinal absorption of short chain fatty acids that do not require packaging into lipoprotein particles for absorption and transport.

Finally, we determined whether knockdown of Mtp expression would affect absorption of dietary lipid (consisting of medium and long chain fatty acid containing TAG) by placing 5 dpf Mtp MO-injected larvae in diluted heavy whipping cream (as in Figure 3) for 6 h. No neutral lipid was seen in the vasculature of Mtp MO-injected larvae after feeding (Figure 5B), although the animals did swallow the food. For comparison, an uninjected, 5 dpf larva is shown (Figure 5B). In summary, Mtp MO injection led to specific malabsorption of dietary TAGs.

DISCUSSION

With improved understanding of how abnormalities in the uptake, transport, and disposition of neutral lipids occur, multiple therapeutic portals for the treatment of illnesses such as obesity, hyperlipidemia, atherosclerosis, hepatic steatosis, and diabetes mellitus can be opened. Via the development of methods for analyzing and monitoring neutral lipids, the transparent, genetically tractable zebrafish larvae would serve as an excellent tool for opening such avenues of research into lipid metabolism. Here, we have used a simple staining method to visualize neutral lipid in zebrafish embryos and larvae during development. In addition to monitoring endotrophic lipid utilization, we were able to assess the fate of dietary lipids and to examine the consequences of targeted knockdown of the central lipoprotein particle processing enzyme Mtp. These studies confirm not only that the lipid processing machinery is ancient and highly conserved but

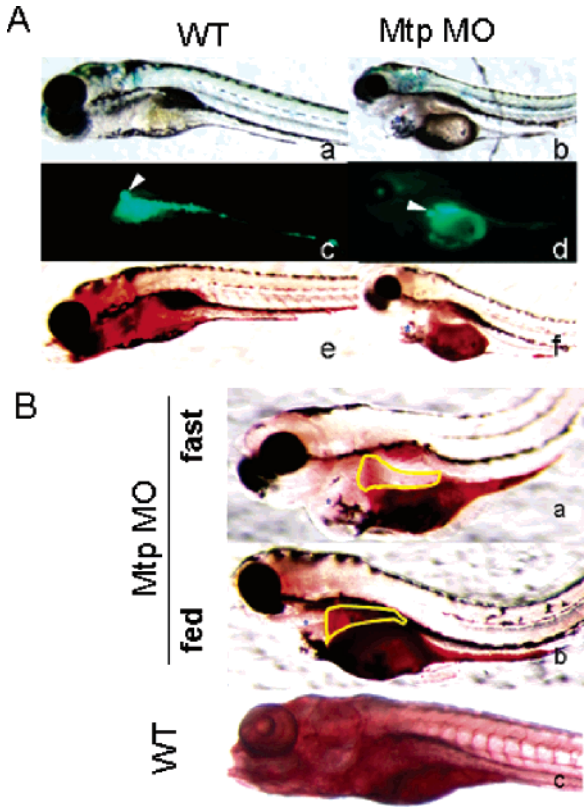

FIGURE 5: Mtp is required for absorption of dietary fat, but not of a short chain fatty acid analogue. (A) WT (a, c, and e) and Mtp MO-injected (b, d, and f) 4 dpf larvae were incubated with PED6 for 24 h. Light (a and b) and green fluorescence (c and d) photomicrographs were taken 24 h later. Larvae were then fixed and stained with ORO (e and f). Note the presence of the liberated short chain fatty acid BODIPY C5 in the gall bladder (arrowhead). Pericardiac edema is noted in the Mtp MO-injected larvae (blue asterisks). (B) Five days postfertilization Mtp MO-injected larvae were maintained in water (a) or incubated for 6 h in diluted whipping cream (b) as in Figure 3. For comparison, an uninjected, 5 dpf embryo is shown (c). Larvae were fixed and stained with ORO. Note the presence of a neutral lipid in the lumen of the anterior intestine of the fed Mtp MO-injected embryo (yellow outline), but the complete absence of a neutral lipid in the vasculature (b).

also that the tools we used and validated here shall allow us to peform an unbiased forward genetic screen to identify mutations causing derangements in lipid transport, storage, and catabolism.

Detecting Neutral Fat in Zebrafish Larvae. BODIPY-modified fatty acids were used successfully in expression cloning of fatty acid transport proteins in cell culture (*20*). Unlike shorter chain fatty acids (like valeric acid and its derivative BODIPY C5), poorly soluble medium and long chain fatty acids require fatty acid binding proteins for intracellular transport, and they must be incorporated into TAG and lipoprotein particles for absorption (*33*). It was our initial hope that these properties would allow us to visualize neutral lipids during embryogenesis by feeding larvae a fluorescently conjugated medium chain fatty acid. Unfortunately, we found that fluorescent analogues of medium chain fatty acids are not suitable for examining the location of neutral lipids in whole larvae because the medium chain fatty acid analogue BODIPY 558/568 C12 was minimally absorbed by the intestine and was not seen in the circulation (Figure 1). This fatty acid analogue and the vital neutral lipid stain nile red were seen predominantly in the intestine several hours after the short chain fatty acid analogue BODIPY C5 is cleared by 6 dpf zebrafish embryonic intestines (*16*). The difference in the efficiency of absorption between the two BODIPY derivatives is due to the length of the fatty acyl moiety (see below). Unfortunately, the efficiency of incorporation of BODIPY derivatives of fatty acids into neutral lipids is low (*21*).

Endotrophic Lipid Utilization and Absorption of Dietary Fat. Because of these limitations of fluorescent lipid derivatives, we stained endogenous lipids with ORO to obtain a complete picture of the neutral lipid dynamics in the developing embryo. For the first 5 dpf, the yolk sac is stained with ORO. From 2 to 5 dpf, the vasculature is similarly stained. Once the yolk is consumed, the vasculature is no longer stained with ORO (Figures 2−5); feeding 6 dpf larvae a high-fat liquid restores lipid staining of the vasculature (Figure 3). This staining is lost once larvae are removed from the high-fat liquid, indicating consumption of the dietary lipid by the tissues. These observations indicate that the dynamic appearance and disappearance of neutral lipid in the vasculature can be monitored easily with ORO. They also suggest that we should be able to identify mutants with abnormal lipid deposition in tissues such as liver and skeletal muscle in a large-scale genetic screen. Furthermore, these qualitative observations correlated with the quantitative increase in whole-larval TAG levels following brief feeding of a high-fat liquid (Figure 3).

Knockdown of Mtp. We verified that Mtp MO injection led to a decreased level of Mtp protein expression using immunoblotting of whole-larval lysates (Figure 4). Loss of zebrafish Mtp expression recapitulates the major findings of $Mtp^{-/-}$ mice: a decreased level of Mtp expression leads to a decreased level of yolk lipid consumption and growth retardation, culminating in embryonic death (*26*). When less Mtp MO was injected, Mtp protein was not knocked down and an intermediate phenotype similar to the "silent" hypobetalipoproteinemia of $Mtp^{+/-}$ or patients with missense mutations in *MTP* causing hypobetalipoproteinemia (*24*, *25*) were not seen. Nevertheless, the phenotypes we observed were not due to secondary defects in cardiovascular development (Figure 4), nor was global intestinal function impaired by Mtp knockdown (Figure 5). Indeed, the upregulation of whole-larval levels of Foxa2 and Pgc1 in Mtp MO-injected fish suggests a coordinated attempt to increase the level of *mtp* expression (*46*) in the face of genetically induced starvation. This specific phenotype—impaired transport of dietary fat consisting of medium and long chain fatty acids, but normal BODIPY C5 processing—leading to malnutrition and death in Mtp MO-injected larvae contrasts with that of *ffr* mutants, which have more generalized vesicular transport defects, despite appearing grossly normal (*18*).

CONCLUSION

Using a simple staining method, we found that zebrafish larvae are suitable for the microscopic and biochemical study of lipid transport. We envision a large-scale genetic screen for defects in lipid uptake, transport, and disposition using this method. An unbiased search for proteins differentially regulated by feeding using whole-organismal proteomic analysis is also underway.

ACKNOWLEDGMENT

We thank Drs. Eric Y. Yen, Malin Levin, and Robert V. Farese, Jr., for advice and help with triacylglycerol assays; Dr. Massimo Santoro for help with *cloche* mutants; Dr. Carol C. Shoulders for the Mtp−PDI IgG; and Dr. Don L. Gibbons, Jr., for reading and improving an earlier draft of the manuscript.

REFERENCES

1. Stahl, A. (2004) A current review of fatty acid transport proteins (SLC27), *Pfluegers Arch. 447*, 722−727.
2. Pohl, J., Ring, A., Ehehalt, R., Herrmann, T., and Stremmel, W. (2004) New concepts of cellular fatty acid uptake: Role of fatty acid transport proteins and of caveolae, *Proc. Nutr. Soc. 63*, 259−262.
3. Haunerland, N. H., and Spener, F. (2004) Fatty acid-binding proteins: Insights from genetic manipulations, *Prog. Lipid Res. 43*, 328−349.
4. Buhman, K. K., Chen, H. C., and Farese, R. V., Jr. (2001) The enzymes of neutral lipid synthesis, *J. Biol. Chem. 276*, 40369−40372.
5. Wetterau, J. R., Combs, K. A., Spinner, S. N., and Joiner, B. J. (1990) Protein disulfide isomerase is a component of the microsomal triglyceride transfer protein complex, *J. Biol. Chem. 265*, 9800−9807.
6. Wu, X., Zhou, M., Huang, L.-S., Wetterau, J., and Ginsberg, H. N. (1996) Demonstration of a physical interaction between microsomal triglyceride transfer protein and apolipoprotein B during the assembly of ApoB-containing lipoproteins, *J. Biol. Chem. 271*, 10277−10281.
7. Shelness, G. S., and Ledford, A. S. (2005) Evolution and mechanism of apolipoprotein B-containing lipoprotein assembly, *Curr. Opin. Lipidol. 16*, 325−332.
8. Sellers, J. A., Hou, L., Athar, H., Hussain, M. M., and Shelness, G. S. (2003) A *Drosophila* microsomal triglyceride transfer protein homolog promotes the assembly and secretion of human apolipoprotien B. Implications for human and insect transport and metabolism, *J. Biol. Chem. 278*, 20367−20373.
9. Sellers, J. A., Hou, L., Schoenberg, D. R., Batistuzzo, de Medeiros, S. R., Wahli, W., and Shelness, G. S. (2005) Microsomal triglyceride transfer protein promotes the secretion of *Xenopus laevis* vitellogenin A1, *J. Biol. Chem. 280*, 13902−13905.
10. Rava, P., Ojakian, G. K., Shelness, G. S., and Hussain, M. M. (2006) Phospholipid transfer activity of microsomal triacylglycerol transfer protein is sufficient for the assembly and secretion of apolipoprotein B lipoproteins, *J. Biol. Chem. 281*, 11019−11027.
11. Marza, E., Barthe, C., André, M., Villeneuve, L., Helou, C., and Babin, P. J. (2005) Developmental expression and nutritional regulation of a zebrafish gene homologous to mammalian microsomal triglyceride transfer protein large subunit, *Dev. Dyn. 232*, 506−518.
12. Hendrickson, H. S., Hendrickson, E. K., Johnson, I. D., and Farber, S. A. (1999) Intramolecularly quenched BODIPY-labeled phospholipid analogs in phospholipase A_2 and platelet-activating factor acetylhydrolase assays and in vivo fluorescence imaging, *Anal. Biochem. 276*, 27−35.
13. Babin, P. J., and Vernier, J. M. (1989) Plasma lipoproteins in fish, *J. Lipid Res. 30*, 467−489.
14. Babin, P. J., Thisse, C., Durliat, M., André, M., Akimenko, M. A., and Thisse, B. (1997) Both apolipoprotein E and A-1 genes are present in a nonmammalian vertebrate and are highly expressed during embryonic development, *Proc. Natl. Acad. Sci. U.S.A. 94*, 8622−8627.
15. André, M., Ando, S., Ballagny, C., Durliat, M., Poupard, G., Briancon, C., and Babin, P. J. (2004) Intestinal fatty acid binding protein gene expression reveals the cephalocaudal patterning during zebrafish gut morphogenesis, *Int. J. Dev. Biol. 44*, 249−252.
16. Farber, S. A., Pack, M., Ho, S. Y., Johnson, I. D., Wagner, D. S., Dosch, R., Mullins, M. C., Hendrickson, H. S., Hendrickson, E. K., and Halpern, M. E. (2001) Genetic analysis of digestive physiology using fluorescent phospholipid reporters, *Science 292*, 1385−1388.
17. Rawls, J. F., Samuel, B. S., and Gordon, J. I. (2004) Gnotobiotic zebrafish reveal evolutionarily conserved responses to the gut microbiota, *Proc. Natl. Acad. Sci. U.S.A. 101*, 4596−4601.
18. Ho, S. Y., Lorent, K., Pack, M., and Farber, S. A. (2006) Zebrafish fat-free is required for intestinal lipid absorption and Golgi apparatus structure, *Cell. Metab. 3*, 289−300.
19. Watanabe, T., Asaka, S., Kitagawa, D., Saito, K., Kurashige, R., Sasado, T., Morinaga, C., Suwa, H., Niwa, K., Henrich, T., Deguchi, T., Iwanami, N., Watanabe, T., Kunimatsu, S., Osakada, M., Okamoto, Y., Kota, Y., Yamnaka, T., Tanaka, M., Kondoh, H., and Furutani-Keiki, M. (2004) Mutations affecting liver development and function in Medaka, Oryzias latipes, screened by multiple criteria, *Mech. Dev. 121*, 791−802.
20. Stahl, A., Hirsch, D. J., Gimeno, R. E., Punreddy, S., Ge, P., Watson, N., Patel, S., Kotler, M., Raimondi, A., Tartaglia, L. A., and Lodish, H. (1999) Identification of the major intestinal fatty acid transport protein, *Mol. Cell 4*, 299−308.
21. Huang, H., Starodub, O., McIntosh, A., Kier, A. B., and Schroeder, F. (2002) Liver fatty acid-binding protein targets fatty acids to the nucleus. Real time confocal and multiphoton fluorescence imaging in living cells, *J. Biol. Chem. 277*, 29139−29151.
22. Mak, H. Y., Nelson, L. S., Basson, M., Johnson, C. D., and Ruvkun, G. (2006) Polygenic control of *Caenorhabditis elegans* fat storage, *Nat. Genet. 38*, 363−368.
23. Hornung, M. W., Cook, P. M., Flynn, K. M., Lothenback, D. B., Johnson, R. D., and Nichols, J. W. (2004) Use of multi-photon laser-scanning microscopy to describe the distribution of xenobiotic chemicals in fish early life stages, *Aquat. Toxicol. 67*, 1−11.
24. Wetterau, J. R., Aggerbeck, L. P., Bouma, M.-E., Eisenberg, C., Munck, A., Hermier, M., Schmitz, J., Gay, G., Rader, D. J., and Gregg, R. E. (1992) Absence of microsomal triglyceride transfer protein in individuals with abetalipoproteinemia, *Science 258*, 999−1001.
25. Sharp, D., Blinderman, L., Combs, K. A., Kienzle, B., Ricci, B., Wager-Smith, K., Gil, C. M., Turck, C. W., Boumas, M.-E., Rader, D. J., Aggerbeck, L. P., Gregg, R. E., Gordon, D. A., and Wtterau, J. R. (1993) Cloning and gene defects in microsomal triglyceride transfer protein associated with abetalipoproteinaemia, *Nature 365*, 65−69.
26. Raabe, M., Flynn, L. M., Zlot, C. H., Wong, J. S., Veniant, M. M., Hamilton, R. L., and Young, S. G. (1998) Knockout of the abetalipoproteinemia gene in mice: Reduced lipoprotein secretion in heterozygotes and embryonic lethality in homozygotes, *Proc. Natl. Acad. Sci. U.S.A. 95*, 8686−8691.
27. Raabe, M., Veniant, M. M., Sullivan, M. A., Zlot, C. H., Bjorkegren, J., Nielsen, L. B., Wong, J. S., Hamilton, R. L., and Young, S. G. (1999) Analysis of the role of microsomal triglyceride transfer protein in the liver of tissue-specific knockout mice, *J. Clin. Invest. 103*, 1287−1298.
28. Chang, B. H., Liao, W., Li, L., Nakamuta, M., Mack, D., and Chan, L. (1999) Liver-specific inactivation of the abetalipoproteinemia gene completely abrogates very low density lipoprotein/low density lipoprotein production in a viable conditional knockout mouse, *J. Biol. Chem. 274*, 6051−6055.
29. Xie, Y., Newberry, E. P., Young, S. G., Robine, S., Hamilton, R. L., Wong, J. S., Luo, J., Kennedy, S., and Davidson, N. O. (2006) Compensatory increase in hepatic lipogenesis in mice with conditional intestine-specific Mttp deficiency, *J. Biol. Chem. 281*, 4075−4086.
30. Westerfield, M. (2000) *The Zebrafish Book. A Guide for the Laboratory Use of Zebrafish (Danio rerio)*, 4th ed., University of Oregon Press, Eugene, OR.
31. Field, H. A., Ober, E. A., Roeser, T., and Stainier, D. Y. (2003) Formation of the digestive system in zebrafish. I. Liver morphogenesis, *Dev. Biol. 253*, 279−290.
32. Jin, S. W., Beis, D., Mitchell, T., Chen, J. N., and Stainier, D. Y. (2005) Cellular and molecular analyses of vascular tube and lumen formation in zebrafish, *Development 132*, 5199−5209.
33. Stainier, D. Y., Weinstein, B. M., Detrich, H. W., III, Zon, L. I., and Fishman, M. C. (1995) Cloche, an early acting zebrafish gene, is required by both the endothelial and hematopoietic lineages, *Development 121*, 3141−3150.
34. Ritchie, P. J., Decout, A., Amey, J., Mann, C. J., Read, J., Rosseneu, M., Scott, J., and Shoulders, C. C. (1999) Baculovirus expression and biochemical characterization of the human microsomal triglyceride transfer protein, *Biochem. J. 338*, 305−310.
35. Schlegel, A., Arvan, P., and Lisanti, M. P. (2001) Caveolin-1 binding to endoplasmic reticulum membranes and entry into the regulated secretory pathway are regulated by serine phosphor-

ylation. Protein sorting at the level of the endoplasmic reticulum, *J. Biol. Chem. 276*, 4398−4408.
36. Snyder, F., and Stephens, N. (1959) A simplified spectrophotometric determination of ester groups in lipids, *Biochim. Biophys. Acta 34*, 244−245.
37. Borradaile, N. M., de Dreu, L. E., Barrett, P. H., Behrsin, C. D., and Huff, M. W. (2003) Hepatocyte ApoB-containing lipoprotein secretion is decreased by the grapefruit flavonoid, naringenin, via inhibition of MTP-mediated microsomal triglyceride accumulation, *Biochemistry 42*, 1283−1291.
38. Sheridan, M. A. (1988) Lipid dynamics in fish: Aspects of absorption, transportation, deposition and mobilization, *Comp. Biochem. Physiol., Part B: Biochem. Mol. Biol. 90*, 679−690.
39. Schlombs, K., Wagner, T., and Scheel, J. (2003) Site-1 protease is required for cartilage development in zebrafish, *Proc. Natl. Acad. Sci. U.S.A. 100*, 14024−14029.
40. Smart, E. J., De Rose, R. A., and Farber, S. A. (2004) Annexin 2-caveolin 1 complex is a target of ezetimibe and regulates intestinal cholesterol transport, *Proc. Natl. Acad. Sci. U.S.A. 101*, 3450−3455.
41. Bennett, A. J., Billett, M. A., Salter, A. M., and White, D. A. (1995) Regulation of hamster hepatic microsomal triglyceride transfer protein mRNA levels by dietary fats, *Biochem. Biophys. Res. Commun. 212*, 473−478.
42. Bennett, A. J., Bruce, J. S., Salter, A. M., White, D. A., and Billett, M. A. (1996) Hepatic microsomal triglyceride transfer protein messenger RNA concentrations are increased by dietary cholesterol in hamsters, *FEBS Lett. 394*, 247−250.
43. Lu, S., Huffman, M., Yao, Y., Mansbach, C. M., II, Cheng, X., Meng, S., and Black, D. D. (2002) Regulation of MTP expression in developing swine, *J. Lipid Res. 43*, 1303−1311.
44. Lin, M. C., Arbeeny, C., Bergquist, K., Kienzle, B., Gordon, D. A., and Wetterau, J. R. (1994) Cloning and regulation of hamster microsomal triglyceride transfer protein. The regulation is independent from that of other hepatic and intestinal proteins which participate in the transport of fatty acids and triglycerides, *J. Biol. Chem. 269*, 29138−29145.
45. Swift, L. L., Jovanovska, A., Kakkad, B., and Ong, D. E. (2005) Microsomal triglyceride transfer protein expression in mouse intestine, *Histochem. Cell Biol. 123*, 475−482.
46. Wolfrum, C., and Stoffel, M. (2006) Coactivation of Foxa2 through Pgc-1β promotes liver fatty acid oxidation and triglyceride/VLDL secretion, *Cell. Metab. 3*, 99−110.

BI0619268